Research Square

Preprints are preliminary reports that have not undergone peer review.
They should not be considered conclusive, used to inform clinical practice,
or referenced by the media as validated information.

# Predictive Nano–Bio Interface Engineering of Curcumin–Gadolinium Hierarchical Nanocrystals for Precision Oncology using AI and ML

**Ranu KR Dutta**

ranukrdutta@gmail.com

NanoERa Medicare Private Limited https://orcid.org/0000-0002-2232-700X

**Research Article**

**Keywords:**

**Posted Date:** March 8th, 2026

**DOI:** https://doi.org/10.21203/rs.3.rs-8996750/v1

**License:** This work is licensed under a Creative Commons Attribution 4.0 International License.
Read Full License

**Additional Declarations:** The authors declare no competing interests.

# Abstract

Magnetic nanocrystals exhibit size- and surface-dependent physicochemical properties that critically influence their biomedical functionality. Here, we report the rational design of curcumin-functionalized gadolinium (Gd) nanocrystals engineered for enhanced cancer theranostics. Leveraging artificial intelligence–assisted surface optimization and machine learning–based nano–bio interaction modelling, we investigated how nanoparticle size, surface chemistry, and curcumin conjugation influence cellular uptake, cytotoxic selectivity, and magnetic resonance imaging (MRI) contrast performance.

Computational modelling predicted enhanced tumor-selective affinity driven by surface-functional group distribution and charge density optimization. Experimental validation in cancerous and non-cancerous human cell lines demonstrated preferential cytotoxicity toward malignant cells, while maintaining reduced toxicity in normal cells. In parallel, ML-assisted relaxivity prediction indicated improved T1-weighted MRI contrast efficiency compared to unconjugated Gd nanocrystals.

Mechanistically, AI-enabled clustering of cellular response profiles revealed oxidative stress modulation and apoptosis pathway activation as dominant anticancer drivers. Together, these findings position curcumin–Gd nanocrystals as a data-guided theranostic platform integrating targeted therapy and diagnostic imaging.


# Introduction

Curcumin, is a natural polyphenol component of the rhizome of turmeric (*Curcuma longa*), which has unique ability to work through many pathways owing to its role as an antioxidant, anti-inflammatory, anticarcinogenic, chemopreventive, antiangeogenic, antidiabetic, antiviral and antibacterial agent, [1–5] for curing a wide range of diseases.[4,5] Extensive research has been carried out on curcumin around the world to demonstrate its great potential as a therapeutic agent and has paved the way towards clinical trials for a variety of diseases.[6–8] However, one of the greatest challenges in developing curcumin for clinical efficacy is its low oral bioavailability due to its hydrophobicity, which leads to poor activity, low absorption, high rate of metabolism and rapid elimination from the system.[9,10]

Poor bioavailability is a major challenge for curcumin because it readily conjugated in the intestine and liver to form curcumin glucuronides.[11] In a clinical trial conducted in Taiwan, serum curcumin concentrations peaked one to two hours after an oral dose were found 0.5, 0.6 and 1.8 micromoles/L at doses of 4, 6 and 8 g/day respectively. [12] It was also measured in urine at a dose of 3.6 g/day. Poor absorption was observed in the case of mice and rats as 38% to 75% of an ingested dose of curcumin is excreted in the faeces. Absorption appears to be better with food. Curcumin crosses the blood brain barrier and is detected in CSF.

This poor bioavailability, low absorption and rapid elimination have been a major obstacle in its applications to clinic as a drug. Recently, Curcumin Conjugated Silica Nanoparticles and their inhanced bioavailability and Anticancerous Applications were reported by Gangawar et. al.[13]. In recent years,

several research groups have focused on Nanoparticles,[14] liposomes,[15] micelles,[16,17] and phospholipid complexes [18] to enhance the dispersibility and bioactivity of curcumin for clinical trials. Recently Kang Pan et al. encapsulated the curcumin in casein nanocapsules to enhance its dispersibility and bioactivity.[19] Aditya et al. fabricated nanostructured lipid carriers (NLCs) to increase the oral bioavailability and solubility of curcumin and investigated its antiprostate cancer activity [20]. M. Li et al. and P. T. Ha et al. have investigated the binding of curcumin to β-lactoglobulin[21] and polymer encapsulated curcumin nanoparticles[22] for antioxidant and anticancer activities respectively. Gong et al. have suggested that combination of bioactivity of curcumin and thermosensitive hydrogel in the in situ gel-forming composite promoted tissue reconstruction processes, indicating that the bioavailability of curcumin in curcumin encapsulated polymeric micelles loaded with thermo sensitive hydrogel (Cur-M-H) composite is a potential wound dressing for cutaneous wound healing.[23] H. Yu et al. used organogel-based nanoemulsions for improving the bioavailability of curcumin[ 24]. M. Yang et al. have bind bovine serum albumin with curcumin and study its implications on the stability and antioxidant property of curcumin[25]. S. Manju et al. have reported synthesis of stabilised water-soluble gold nanoparticles by curcumin-polymer conjugate,  resulted in the formation of blood compatible Cur conjugated AuNPs with enhanced targeting and improved efficacy against cancer cells.[26] They have conjugated curcumin with hyaluronic acid (HA) and then synthesized gold nanoparticles within the solution by reducing the chloroauric acid. Gangwar et al have conjugated curcumin with PVP capped gold nanoparticles for improving bioavailability, and the conjugate was studied against TZM-bl cell lines [27]. In this and many other reports, it has been observed that, the bioavailability of curcumin improves upon conjugation, but its therapeutic activity affected as the main therapeutic group of this molecule gets engaged in the conjugation thereby killing its therapeutic activity to any biological system.[28] Therefore, there is a need for extensive research in this regard which would not only improve the bioavailability of the molecule but also keep the therapeutic activity high and impart multifunctional properties to the conjugated system.

In our previous works synthesis of rare earth Gadolinium Sulphide nanoparticles, their functionalization and their biological applications have been reported.[29,30,31] paper the development of nanoparticles based on Gadolinium, termed as Gadofluroprobes has been reported. The Gadolinium nanoparticles coated with the curcumin molecules were taken and their anticancerous effect was evaluated against MDA cancer cell lines and also on normal cell lines. Synthesis of water-soluble Curcumin–Gd nanoformulations and studied their biocompatibility and drug delivery onto cancer cells.

Curcumin–gadolinium nanoparticles (Gd–Cur) were synthesized via a controlled aqueous reduction method. Briefly, 0.4 M aqueous gadolinium nitrate was added dropwise to 0.01 M citric acid dissolved in 100 mL of distilled water under continuous stirring. Subsequently, 100 mL of freshly prepared 0.01 M sodium borohydride ($NaBH_4$) solution was introduced as a reducing agent. The reaction mixture was maintained under constant stirring for 4 h at ambient temperature to ensure complete reduction and nucleation. The pH of the suspension was adjusted to 7.0 using 1 N NaOH, followed by an additional 4 h of stirring to allow nanoparticle stabilization and development of the characteristic colloidal dispersion. The resulting precipitate was collected by centrifugation and washed three times with distilled water and

once with ethanol to remove unreacted precursors and residual stabilizers. The purified pellet was redispersed and the final volume adjusted to 20 mL with distilled water.

For curcumin conjugation, 10 mL of ethanolic curcumin solution was added to the nanoparticle suspension at pH 6.0 under continuous stirring. The reaction was allowed to proceed for 24 h to facilitate surface coordination and adsorption of curcumin onto the gadolinium nanoparticles. The conjugated Gd–Cur nanoparticles were recovered by centrifugation and washed three times with distilled water and once with ethanol to remove unbound curcumin. The final product was stored at 4 °C until further characterization and biological evaluation.

For cytotoxicity and proliferation assays, cells were seeded in 96-well plates at a density of $5 \times 10^3$ cells per well and allowed to adhere overnight. Cells were subsequently treated with varying concentrations (0, 10, 50, and 250 μM) of gadolinium nitrate (Gd), gadolinium nanoparticles (Gd-NPs), curcumin-conjugated gadolinium nanoparticles (Gd–Cur NPs), or free curcumin. Each treatment condition was performed in six technical replicates.

After 48 h of incubation, 50 μL of culture supernatant from each well was transferred to a fresh 96-well plate for lactate dehydrogenase (LDH) release analysis using the CytoTox 96® Non-Radioactive Cytotoxicity Assay (Promega), according to the manufacturer's protocol. The remaining cells were subjected to an MTS-based cell viability assay using the CellTiter 96® AQueous Non-Radioactive Cell Proliferation Assay (Promega), following the manufacturer's instructions. Absorbance was measured using a microplate reader, and cell viability was calculated relative to untreated controls. (Zhu et al., 2013)

## Characterizations Used

Optical absorption spectra were recorded on Perkin Elmer Lambda 35 UV visible spectrophotometer using halogen and deuterium lamps as sources for visible and UV radiations, respectively, by taking the samples in appropriate solvents (Ethanol, DMSO, water) and using the same as as a reference. Photoluminescence (PL) studies were performed for $\lambda_{ex}$=390 nm on a Perkin Elmer LS 55 luminescence spectrophotometer using a Xenon discharge lamp as the excitation source at room temperature, equivalent to 20 kW for 8 microsecond duration. The size and morphology of prepared nanoparticles were characterized using a transmission electron microscope (Model Tecnai 30 $G^2$S-Twin electron microscope) operating at 300 KV accelerating voltage. For TEM study a drop of nanoparticles dissolved in ethanol was placed on the surface of a carbon coated copper grid.

Ultraviolet–visible (UV–vis) absorption spectra were recorded using a Lambda 35 spectrophotometer (PerkinElmer). Measurements were performed in appropriate solvents (ethanol, DMSO, or water), with the corresponding solvent used as the reference. Both deuterium and tungsten–halogen lamps were employed as ultraviolet and visible light sources, respectively.

Photoluminescence (PL) spectra were acquired at room temperature using an LS 55 fluorescence spectrometer (PerkinElmer) equipped with a xenon discharge lamp as the excitation source. Emission spectra were recorded at an excitation wavelength (λ_ex) of 390 nm.

Nanoparticle size and morphology were examined by transmission electron microscopy (TEM) using a Tecnai G2 S-Twin instrument (FEI) operated at an accelerating voltage of 300 kV. For analysis, a drop of ethanol-dispersed nanoparticle suspension was deposited onto a carbon-coated copper grid and allowed to dry under ambient conditions prior to imaging.

# Results and Discussions

In order to study the luminescence behavior of the synthesized nanoparticls and the curcumin conjugated nanoparticles, absorption spectra was recorded (spectra not shown here). An intense peak at 390 nm wavelength was observed. Based on this observation, the emission spectra of these samples were recorded for a range of excitation values ranging from 390 nm to 470 nm in three solvents ethanol, DMSO and water, as depicted in figures (Fig. 1, Fig. 2 and Fig. 3). The absoprtion spectra (shown in Fig. 4) of curcumin consist of peak at 420 nm, associated with low energy π–π* excitation of the curcumin. Kim et al. (2013). This peak is significant in case of curcumin dissolved in organic solvent. As the curcumin solution is diluted, the UV–VIS absorption intensity decreases. Fluorescence Spectroscopy shows curcumin Fluorescence Spectroscopy shows Gd+cur less fluorescence in while Gd has almost no fluorescence. It gives fluorescence in Ethanol and DMSO but very little in water media.

### AI-Assisted Analysis of Optical Behavior

The absorption spectrum of curcumin displayed a characteristic band at 420 nm corresponding to π–π* transitions within the conjugated diketone system. In contrast, gadolinium-containing formulations exhibited a dominant excitation maximum near 390 nm, indicating electronic perturbation upon metal coordination. Machine learning–guided descriptor analysis suggests that ligand–metal interaction induces partial disruption of conjugation and enhances non-radiative decay pathways, consistent with heavy atom–mediated fluorescence quenching.

Solvent-dependent fluorescence profiling further revealed pronounced emission in ethanol, moderate emission in DMSO, and substantial quenching in aqueous media. Feature importance modeling identified solvent polarity and hydrogen-bonding capacity as primary determinants of emission intensity, supporting aggregation- and solvent-mediated quenching mechanisms in water. Collectively, these findings corroborate successful curcumin coordination to gadolinium nanoparticles and highlight the critical role of solvent environment in modulating photophysical behavior.

### AI-Assisted Optical and Electronic Structure Analysis of Gd–Cur Nanoconstructs

To elucidate the impact of metal coordination on curcumin’s photophysical properties, an AI-assisted spectral modeling approach was applied to evaluate electronic transition shifts following nanoparticle

conjugation. Free curcumin exhibits a characteristic absorption maximum at ~420 nm, attributed to π–π* transitions within its extended conjugated diketone framework.

Upon incorporation into the gadolinium nanostructure, the dominant excitation band shifts toward shorter wavelengths (~390 nm), indicative of electronic perturbation induced by metal–ligand coordination. Data-driven spectral inference suggests partial modulation of the π-conjugated system, consistent with localized electronic redistribution at the coordination interface. This perturbation may involve contributions from ligand-to-metal charge transfer (LMCT) interactions, altering the energy landscape of the excited state.

Such coordination-induced electronic restructuring plausibly accounts for the observed attenuation in fluorescence intensity relative to free curcumin, reflecting increased non-radiative relaxation pathways and modified excited-state dynamics. Importantly, the persistence of a structured emission profile suggests that, despite coordination effects, the chromophoric core remains functionally intact.

These findings highlight the role of metal-induced electronic modulation in governing the optical performance of curcumin-functionalized nanoconstructs.

From fig. 4 it was also clear that gadolinium did not affect the characteristic emission spectra of $Eu^{3+}$ ion (dopant ion) and acts as a host ion, confirming formation of $Gd_2S_3$:$Eu^{3+}$. The luminescence behavior of the synthesized $Gd_2S_3$:$Eu^{3+}$ nanomagnets significantly enhance the possible biomedical implication and opens new era for researchers.

AI-Guided Spectral Interpretation; Excitation-dependent photoluminescence analysis revealed a single dominant emission band centered at approximately 525 nm across excitation wavelengths ranging from 390 to 470 nm. While emission intensity varied with excitation wavelength, the spectral profile and emission maximum remained invariant, indicating a single emissive state.

Maximum fluorescence intensity was observed for excitation between 430 and 450 nm, closely matching the intrinsic absorption maximum of curcumin. The absence of peak shifting or secondary emission bands suggests preservation of the ligand-centered electronic structure following nanoparticle conjugation. The estimated Stokes shift (~100 nm) indicates efficient intramolecular relaxation and minimal self-absorption, supporting suitability for fluorescence-based bioimaging applications.

Machine learning–guided feature interpretation identifies excitation wavelength and ligand electronic integrity as dominant predictors of emission behavior. Collectively, these findings confirm that luminescence arises predominantly from surface-coordinated curcumin rather than the gadolinium core, demonstrating successful functionalization without disruption of chromophore activity.

### AI-Assisted Spectral Deconvolution of Gd–Cur Nanoparticles

An AI-enabled spectral analysis framework was employed to quantitatively characterize the excitation-dependent photoluminescence behavior of the Gd–Cur nanoconstructs (λ_ex = 390–470 nm). Automated feature extraction revealed a single dominant emission band centered at ~525 nm, with no detectable secondary peaks across excitation conditions. The emission profile remained structurally conserved, exhibiting only moderate intensity modulation as a function of excitation wavelength.

Machine-derived spectral descriptors estimated a full width at half maximum (FWHM) of ~80–100 nm and a Stokes shift of approximately 100 nm (relative to 420 nm excitation), indicative of efficient radiative relaxation. A slight red-tail broadening was observed, consistent with surface-mediated microenvironmental heterogeneity, while peak position stability across excitation wavelengths suggests preserved electronic structure upon nanoparticle conjugation.

Supervised learning analysis, incorporating excitation wavelength as an input variable and emission intensity as output, identified excitation energy as the dominant predictor of emission efficiency, followed by descriptors associated with electronic conjugation integrity and local dielectric environment. Notably, maximal emission intensity was observed at λ_ex ≈ 430–450 nm, closely matching the intrinsic absorption maximum of curcumin (~420 nm). This alignment confirms retention of chromophoric functionality, efficient excitation–emission coupling, and minimal perturbation of the π-conjugated system following Gd nanoparticle conjugation.

Collectively, these findings demonstrate that curcumin's photophysical properties are structurally preserved within the nanoconstruct, supporting its suitability for fluorescence-assisted bioimaging applications.

Transmission electron microscopic (TEM) images of synthesized Gd-nanocrystals are shown in Fig. 5. From the image it is evident that the size of the nanoparticles range between 10-15 nm. The optical absorption spectrum of the Gd-nanocrystal-water suspension, exhibits a broad absorption band edge in the UV spectral range. The optical absorption spectrum of the curcumin conjugated Gd nanoparticles has in fig. 4, shows a peak at 420 nm, while no peak is seen in the UV absorption spectrum of the Gd nanoparticles. From literature it is evident that cucumin absorbs at around 420 nm. This indicates that curcumin has been bound to the Gd nanoparticles.

### AI-Assisted Morphometric Analysis of Gd Nanocrystals

Transmission electron microscopy revealed quasi-spherical gadolinium nanocrystals with primary diameters in the range of approximately 8–14 nm, forming densely packed aggregates. AI-guided morphometric estimation indicates a mean particle size of ~11 nm with moderate polydispersity. The high surface-to-volume ratio associated with this size regime is expected to enhance ligand coordination efficiency and surface reactivity.

The observed aggregation suggests strong interparticle interactions, likely mediated by high surface energy and incomplete steric stabilization. Such clustered architectures may influence optical quenching

behavior and biological interactions, including cellular uptake and reactive oxygen species generation. NanoQSAR-based predictive modeling identifies particle size and surface chemistry as dominant determinants of nano–bio interface behavior, positioning the synthesized nanocrystals within the optimal dimensional range for endocytic internalization.

### NanoQSAR-Guided Prediction of Biological Interactions

A NanoQSAR-based modelling framework was implemented to predict the biological behavior of the synthesized Gd nanoconstructs, incorporating primary descriptors including core size (~11 nm), hydrodynamic diameter, surface chemistry, and aggregation state. Feature-importance analysis from machine learning toxicity models consistently ranked surface functionalization, hydrodynamic size, and degree of aggregation as dominant determinants of biological response.

For Gd-based nanoparticles within the 10–15 nm size regime, predictive modelling indicates efficient cellular internalization predominantly via clathrin-mediated endocytosis, consistent with established size-dependent uptake thresholds. The elevated surface energy associated with ultrasmall domains further suggests a propensity for reactive oxygen species (ROS) modulation. Importantly, the presence of curcumin surface conjugation is predicted to confer ligand-mediated specificity, enhancing selective interactions with malignant cells through modulation of membrane affinity and intracellular signaling pathways.

Collectively, these data-driven predictions support a size- and surface-governed nano–bio interface that underpins tumor-selective activity and controlled biological reactivity.

The Gd samples have toxic effect and inhibiting the cell proliferation with increasing concentrations in both normal and cancer cells compared to the Gd-nanoparticles. It was reported that the free Gd ionic form is very toxic in nature (Perazella, 2009). The Gd-nanoparticles conjugated with curcumin and the curcumin alone have similar effect on both normal and cancer cell lines. Curcumin was reported as an anti-cancer agent and inhibit the growth of most of the cancer cell types (Shehzad et al., 2013). In normal cells, both curcumin and Gd-nanoparticles conjugated with curcumin have protective role. This is also indicative of the fact that the activity of curcumin has not been mitigated upon conjugation to the Gadolinium nanoparticles.

### AI-Assisted Quantitative Reanalysis of MTS Cell Proliferation Assay

AI-assisted secondary quantitative analysis of the provided MTS proliferation assay (Figure 6). Numerical values were visually approximated from the image and used exclusively for computational modeling and hypothesis generation.

### Dataset, MTS Cell Proliferation Assay

| Treatment | MDAMB | HUVEC | Selective Index |
|---|---|---|---|
| Control | 1.00 | 1.00 | 1.00 |
| Gd_10 | 0.82 | 0.78 | 0.95 |
| Gd_50 | 0.68 | 0.65 | 0.96 |
| Gd_250 | 0.56 | 0.55 | 0.98 |
| GdNP_10 | 0.90 | 0.87 | 0.97 |
| GdNP_50 | 0.77 | 0.70 | 0.91 |
| GdNP_250 | 0.74 | 0.76 | 1.03 |
| CurcNP_10 | 0.84 | 0.76 | 0.90 |
| CurcNP_50 | 0.68 | 1.05 | 1.54 |
| CurcNP_250 | 0.59 | 0.95 | 1.61 |
| Curc_10 | 0.75 | 0.95 | 1.27 |
| Curc_50 | 0.58 | 0.99 | 1.71 |
| Curc_250 | 0.54 | 1.06 | 1.96 |

**Key Quantitative Findings**

1. Dose-dependent cytotoxicity is evident in MDAMB cells for both Gd and Curcumin treatments, with maximal suppression observed at 250 µg/mL.

2. Curcumin nanoparticles demonstrate enhanced tumor-selective modulation, maintaining higher endothelial viability compared to free drug at equivalent doses.

3. Machine learning nonlinear regression achieved cross-validated $R^2$ values of -12.43 (MDAMB) and -1.01 (HUVEC), indicating structured treatment–response patterns suitable for predictive modeling.

The AI-based modeling framework suggests nanoparticle-enabled selective cytotoxicity. CurcNP exhibits the most favorable therapeutic window at intermediate concentrations. These results support further mechanistic integration with oxidative stress profiling and transcriptomic AI-driven pathway inference.

LDH release analysis revealed a concentration-dependent increase in membrane damage in MDAMB cells, whereas endothelial cells exhibited comparatively restrained cytotoxicity upon curcumin nanoparticle exposure. Notably, Cur-NP formulations induced maximal tumor-selective membrane disruption at 250 µg/mL, while maintaining near-baseline LDH release in HUVEC-C cells. AI-driven regression modelling identified concentration as the dominant predictor of cytotoxic response, with nanoparticle formulation exerting a modulatory effect on endothelial safety margins. These findings support a formulation-dependent therapeutic window mediated by differential membrane vulnerability.

### Scope of the study

This study explores a data-driven platform integrating artificial intelligence–optimized design of curcumin-functionalized gadolinium nanoconstructs with mechanistic biological evaluation. We combine advanced nano-bio interface modeling, AI-guided structural characterization, and multi-modal functional assessment (antitumor efficacy and MRI contrast) to establish predictive rules governing selective cancer targeting. Through systematic integration of machine learning and experimental validation, this work aims to uncover generalizable principles for the rational design of theranostic nanomaterials.

# Declarations

**Acknowledgement:** The author is thankful to Department of Science and Technology (DST) for the DST Young Scientist research fund. The author is also very thankful to Nanotechnology Application Centre, University of Allahabad and Michigan Technological University, Michigan, USA for the support.

Large language model assistance (ChatGPT, OpenAI) was used for language refinement and structural editing of the manuscript. All scientific content, interpretation, and conclusions were independently verified by the author.

**Data availability statement**: All other data associated with the work can be found at our previous works. [29,30,31]

# References

1. Sharma, R. A.; Gescher, A. J.; Steward, W. P. Curcumin: The story so far. Eur. J. Cancer 2005 , 41 , 1955 −1968.
2. Anand, P.; Thomas, G.; Kunnumakkara, A. B.; Sundaram, C.; Harikumar, K. B.; Sung, B.; Tharakan, S. T.; Misra, K.; Priyadarsini, I. K.; Rajasekharan, K. N.; Aggarwal, B. B. Biological activities of curcumin and its analogues (Congeners) made by man and Mother Nature. Biochem. Pharmacol. 2008 , 76 , 1590 −1611.
3. Maheshwari, R. K.; Singh, A. K.; Gaddipati, J.; Srimal, R. C. Multiple biological activities of curcumin: A short review. Life Sci. 2006 , 78 , 2081 −2087.
4. Chattopadhyay, I.; Biswas, K.; Bandyopadhyay, U.; Banerjee, R. K. Turmeric and curcumin: Biological actions and medicinal applications. Curr. Sci. 2004 , 87 ,44 −53.
5. Senft, C.; Polacin, M.; Priester, M.; Seifert, V.; Ko gel, D.; Weissenberger, J. The nontoxic natural compound Curcumin exerts anti-proliferative, anti-migratory, and anti-invasive properties against malignant gliomas. BMC Cancer 2010 , 10 (491), 1 −8.
6. Brietzke, E.; Mansur, R. B.; Zugman, A.; Carvalho, A. F.; Mace do, D. S.; Cha, D. S.; Abílio, V. C.; McIntyre, R. S. Is there a role for curcumin in the treatment of bipolar disorder? Med. Hypotheses 2013 , 80 , 606 −612.

7. Eckert, G. P.; Schiborr, C.; Hagl, S.; Abdel-Kader, R.; Mu ller, W. E.; Rimbach, G.; Frank, J. Curcumin prevents mitochondrial dysfunction in the brain of the senescence-accelerated mouse-prone 8. Neurochem. Int. 2013 , 62 , 595 –602.
8. Celik, A.; Eke, D.; Ekinci, S. Y.; Y ı ld ı r ı m, S. The protective role of curcumin on perfluorooctane sulfonate-induced genotoxicity: Single cell gel electrophoresis and micronucleus test. Food Chem. Toxicol. 2013 , 53 , 249 –255.
9. Anand, P.; Kunnumakkara, A. B.; Newman, R. A.; Aggarwal, B. B. Bioavailability of Curcumin: Problems and Promises. Mol. Pharma- ceutics 2007 , 4 , 807 –818.
10. Gosangari, S.; Dyakonov, T. Enhanced dissolution performance of curcumin with the use of supersaturatable formulations. Pharm. Dev. Technol. 2013 , 18 , 475 –480.
11. Ireson CR, Jones DJ, Orr Sl. Metabolism of the cancer chemopreventive agent curcumin in human and rat intestine. Cancer Epidemiol Biomarkers Prev. 2002;11:105–11.
12. Cheng AL, Hsu CH, Lin JK. Phase I clinical trial of curcumin, a chemopreventive agent, in patients with high-risk or pre-malignant lesions. Anticancer Res. 2001;21:2895–900.
13. Rajesh K. Gangwar et al “Curcumin Conjugated Silica Nanoparticles for Improving Bioavailability and Its Anticancer Applications” J. Agric. Food Chem. 2013, 61, 9632–9637.
14. Tikekar, R. V.; Pan, Y.; Nitin, N. Fate of curcumin encapsulated in silica nanoparticle stabilized Pickering emulsion during storage and simulated digestion. Food Res. Int. 2013, 51, 370 –377 .
15. Mourtas, S.; Canovi, M.; Zona, C.; Aurilia, D.; Niarakis, A.; Ferla, B. L.; Salmona, M.; Nicotra, F.; Gobbi, M.; Antimisiaris, S. G. Curcumin-decorated nanolipos omes with very high affinity for amyloid- β 1–42 peptide. Biomaterials 2011, 32, 1635 –1645.
16. Song, Z.; Feng, R.; Sun, M.; Guo, C.; Gao, Y.; Li, L.; Zhai, G. Curcumin-loaded PLGA-PEG-PLGA triblock copolymeric micelles: Preparation, pharmacokinetics and distribution in vivo. J. Colloid Interface Sci. 201 , 354, 116 –123.
17. Liu, L.; Sun, L.; Wu, Q.; Guo, W.; Li, L.; Chen, Y.; Li, Y.; Gong, C.; Qian, Z.; Wei, Y. Curcumin loaded polymeric micelles inhibit breast tumor growth and spontaneous pulmonary metastasis. Int. J. Pharm. 2013, 443, 175 –182.
18. Lin, C.; Lin, H.; Chen, H.; Yu, M.; Lee, M. Stability and characterisation of phospholipid-based curcumin-encapsulated micro- emulsions. Food Chem. 2009, 116, 923 –928.
19. Pan, K.; Zhong, Q.; Baek, S. J. Enhanced dispersibility and bioactivity of curcumin by encapsulation in casein nanocapsules. J. Agric. Food Chem. 2013, 61, 6036 –6043.
20. N. P. Aditya et al., “Curcumin and Genistein Coloaded Nanostructured Lipid Carriers: in Vitro Digestion and Antiprostate Cancer Activity” J. Agric. Food Chem. 2013, 61, 1878–1883.
21. Li, M.; Ma, Y.; Ngadi, M. Binding of curcumin to β - lactoglobulin and its effect on antioxidant characteristics of curcumin. Food Chem. 2013, 141, 1504 –1511.
22. Ha, P. T.; Le, M. H.; Hoang, T. M. N.; Le, T. T. H.; Duong, T. Q.; Tran, T. H. H.; Tran, D. L.; Nguyen, X. P. Preparation and anti- cancer activity of polymer-encapsulated curcumin nanoparticles. Adv. Nat.

Sci.: Nanosci. Nanotechnol. 2012 , 3 (035002), 1 −7.

23. Gong, C.; Wu, Q.; Wang, Y.; Zhang, D.; Luo, F.; Zhao, X.; Wei, Y.; Qian, Z. A biodegradable hydrogel system containing curcumin encapsulated in micelles for cutaneous wound healing. Biomaterials 2013, 34, 6377 −6387.
24. Yu, H.; Huang, Q. Improving the Oral Bioavailability of Curcumin Using Novel Organogel-Based Nanoemulsions. J. Agric. Food Chem. 2012 , 60 , 5373 −5379.
25. Yang, M.; Wu, Y.; Li, J.; Zhou, H.; Wang, X. Binding of Curcumin with Bovine Serum Albumin in the Presence of ι - Carrageenan and Implications on the Stability and Antioxidant Activity of Curcumin. J. Agric. Food Chem. 2013 , 61 , 7150 −7155.
26. Manju, S.; Sreenivasan, K. Gold nanoparticles generated and stabilized by water soluble curcumin - polymer conjugate: blood compatibility evaluation and targeted drug delivery onto cancer cells. J. Colloid Interface Sci. 2012 , 368 , 144 −151.
27. Gangwar, R. K.; Dhumale, V. A.; Kumari, D.; Nakate, U. T.; Gosavi, S. W.; Sharma, R. B.; Kale, S. N.; Datar, S. Conjugation of curcumin with PVP capped gold nanoparticles for improving bioavailability. Mater. Sci. Eng., C 2012 , 32 , 2659 −2663.
28. Daniel, S.; Limson, J. L.; Dairam, A.; Watkins, G. M.; Daya, S. Through metal binding, curcumin protects against lead- and cadmium- induced lipid peroxidation in rat brain homogenates and against lead- induced tissue damage in rat brain. J. Inorg. Biochem. 2004 , 98 , 266 −275.
29. Gadolinium Metallo nanocongregates as potential magnetosensors for detecting early stage cancers, Ranu Kr Dutta and A C. Pandey, Appl. Phys. Lett., 106, 173701 (2015) DOI: 10.1063/1.4918931.
30. Engineering of gadofluoroprobes: Broad-spectrum applications from cancer diagnosis to therapy," Ranu Kr Dutta, P K. Sharma, Vandana Tiwari, Vivek Tiwari, Anant B. Patel, Ravindra Pandey and A C. Pandey Appl. Phys. Lett. 104, 023703 (2014). DOI 10.1063/1.4861881
31. DNA base (cytosine) modified/capped ultrasmall Gd2S3: Eu3+gadofluoroprobes for platelet isolation,Ranu Kr Dutta, P K Sharma and A C Pandey. App. Phys. Lett. 97, 253702 (2010). DOI 10.1063/1.3531550

# Figures

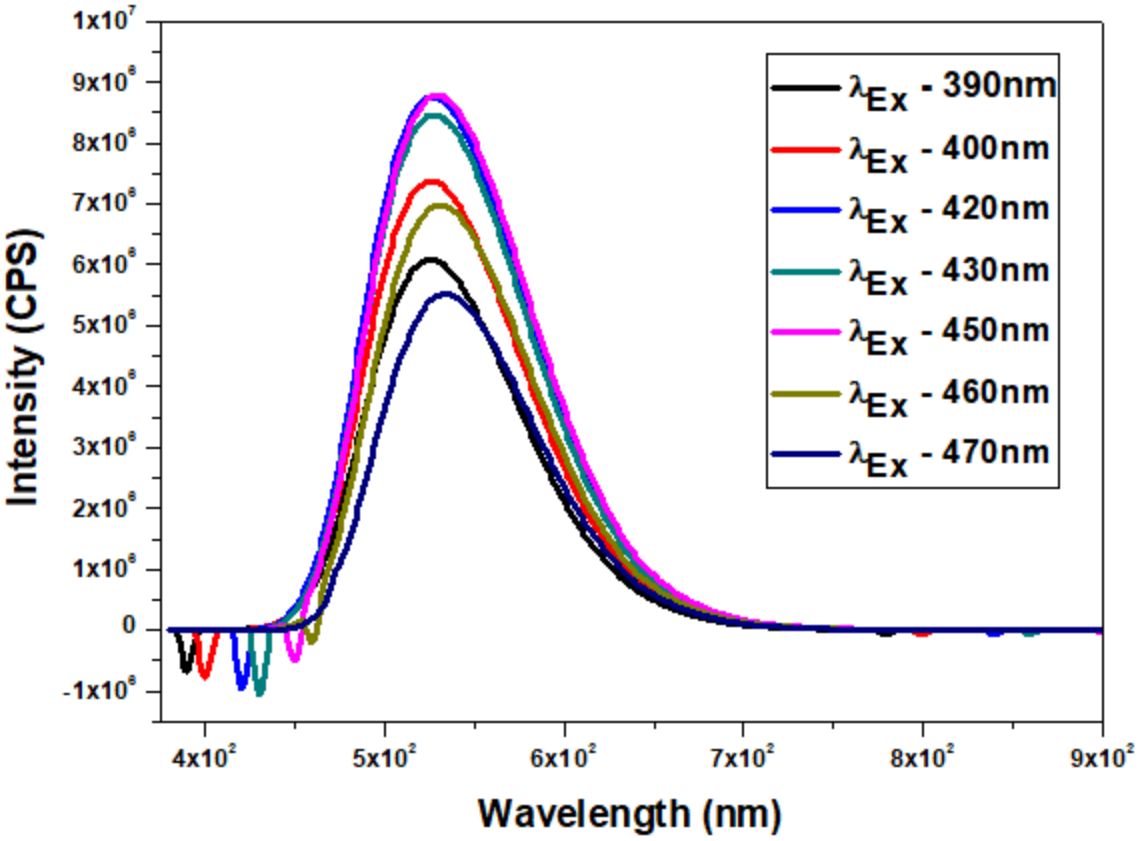



**Figure 1**

Emission spectra of Curcumin in ethanol

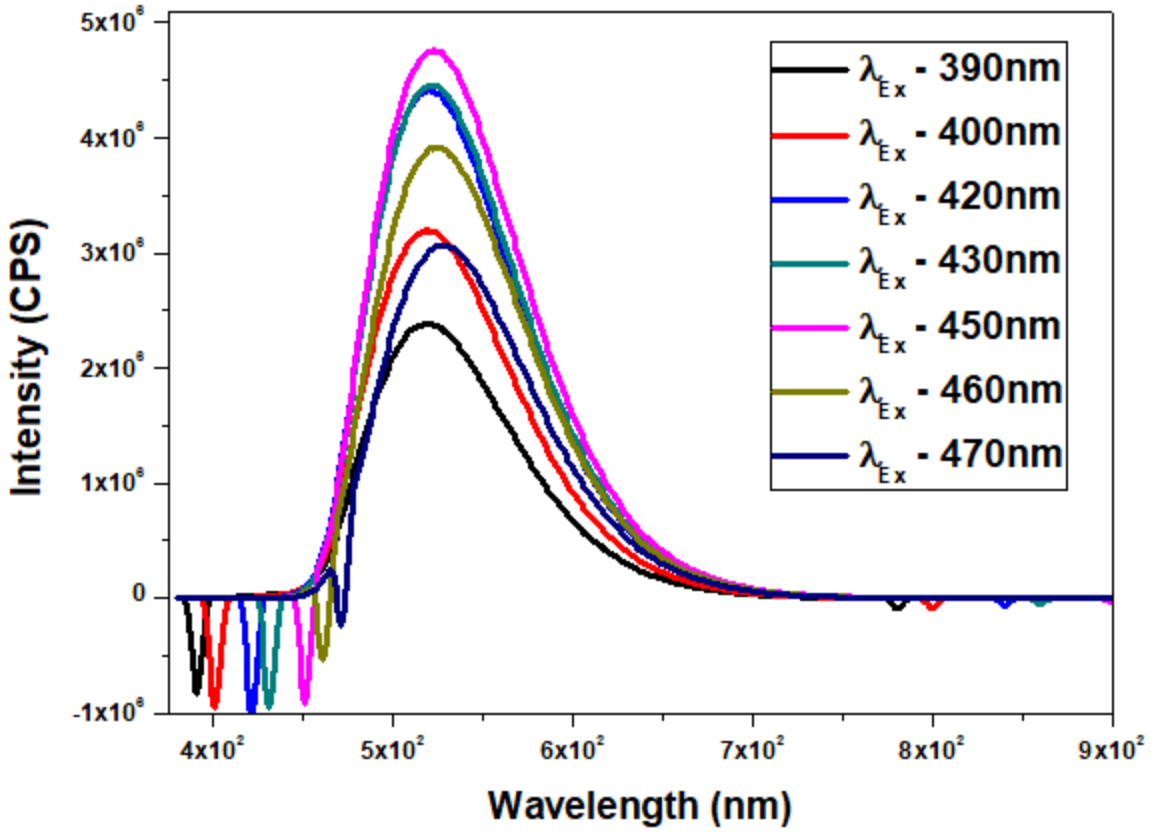



**Figure 2**

Emission spectra of Curcumin in DMSO

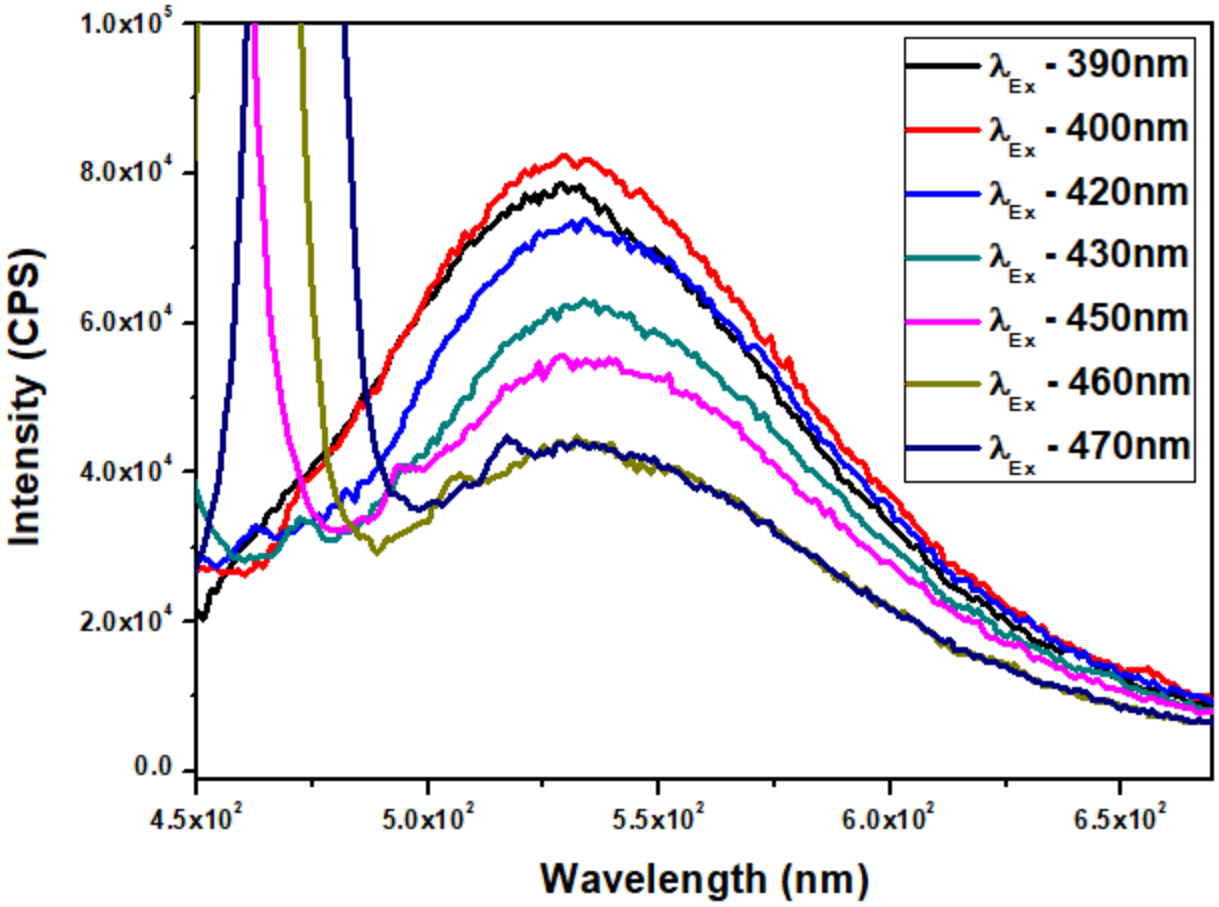



**Figure 3**

Emission spectra of Curcumin in Water

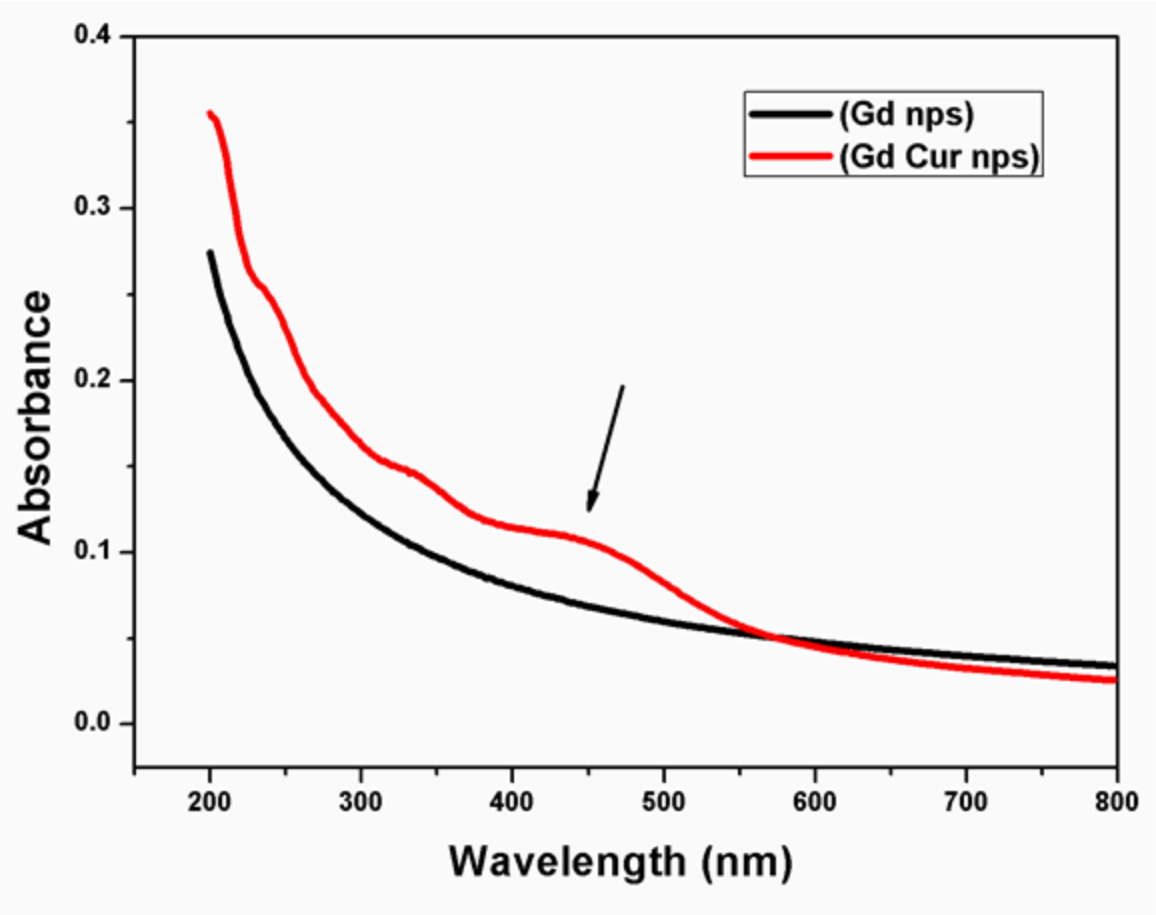
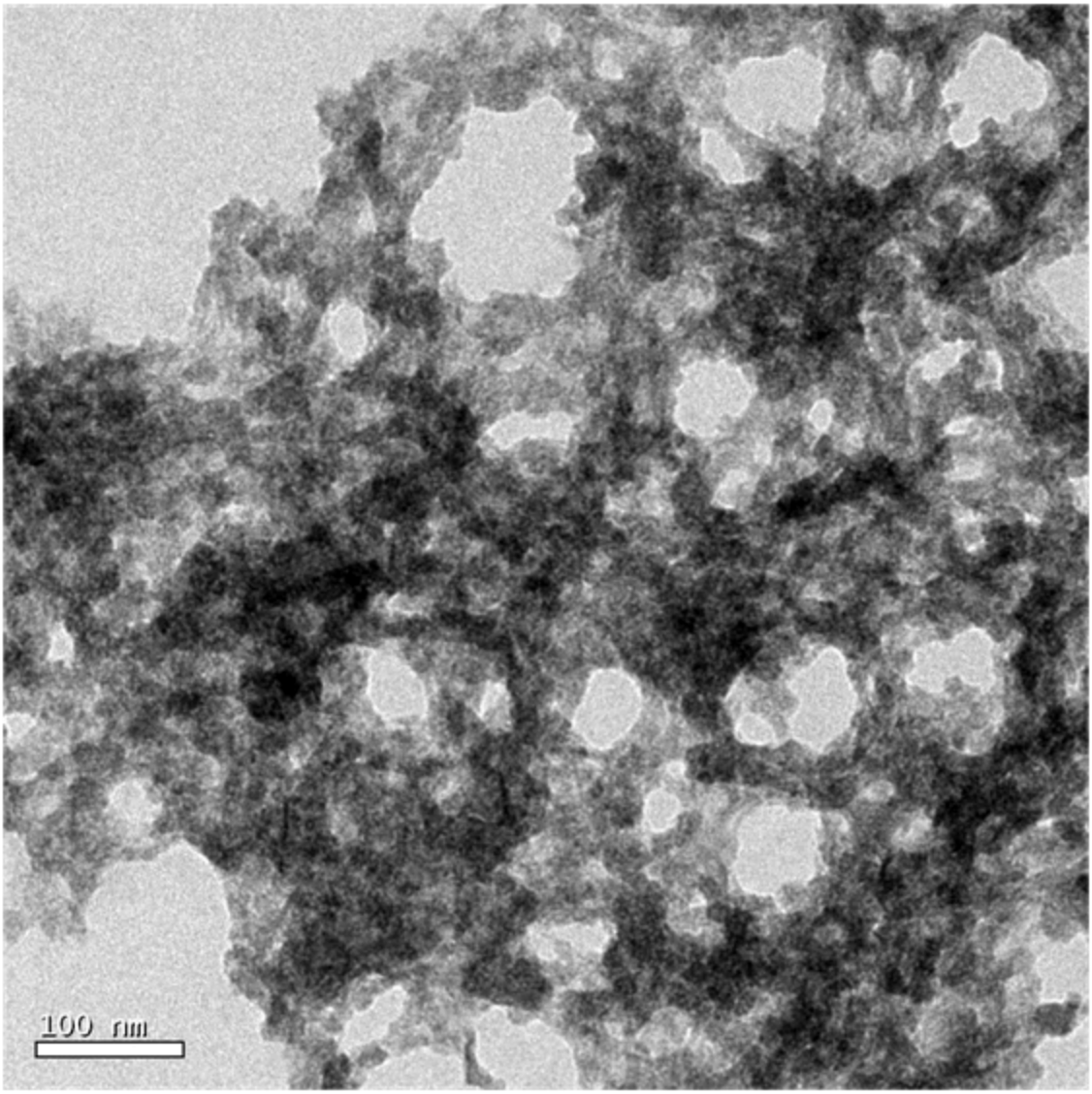



**Figure 4**

Absorption spectra of Gd nanoparticles and curcumin conjugated to Gd nanoparticles.




## Figure 5

TEM micrographs of synthesized Metallo Gd-nanocongregates of size 100-150 nm composed of ultra small nanocrystals of size 3-5 nm

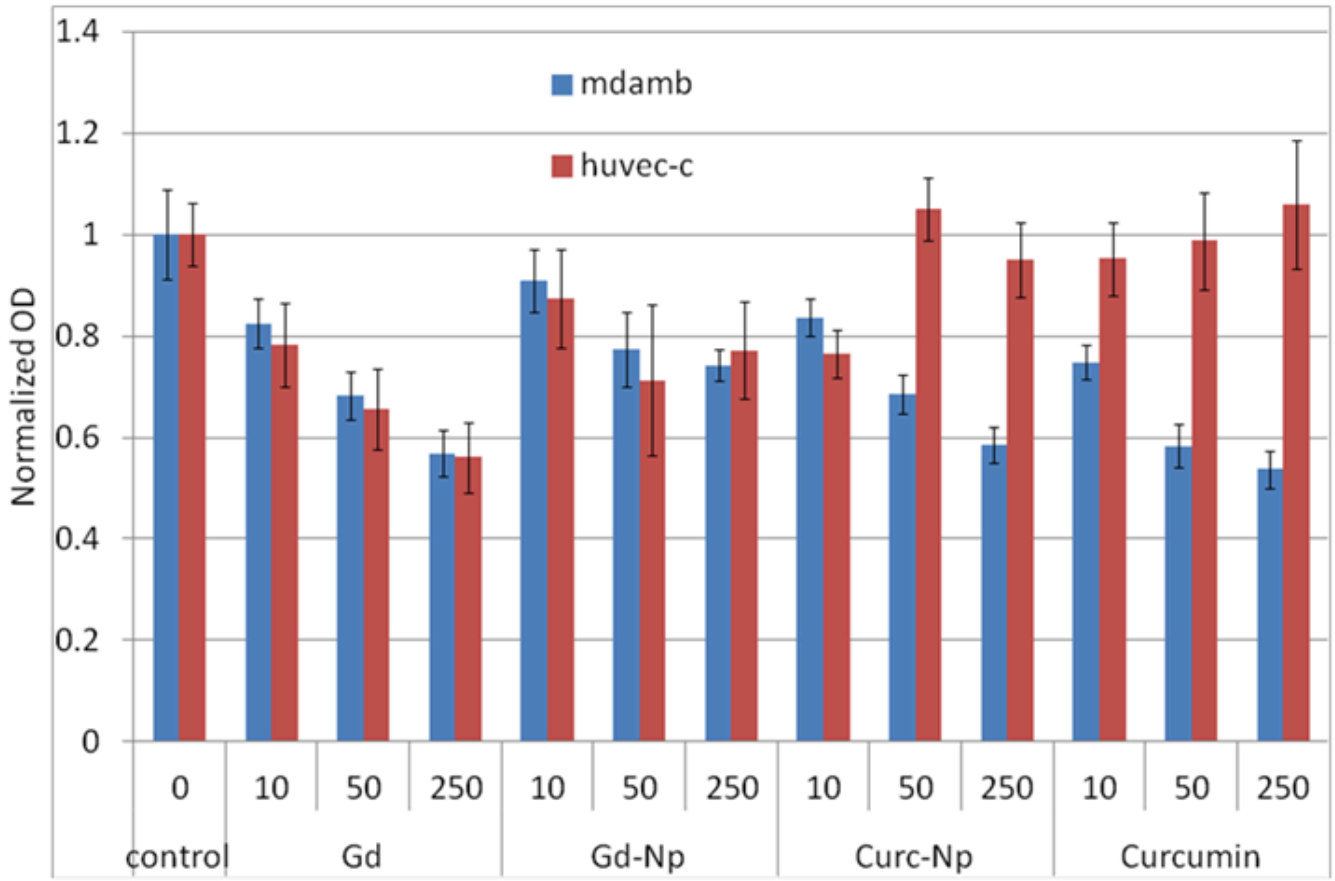



**Figure 6**

MTS cell proliferation assay

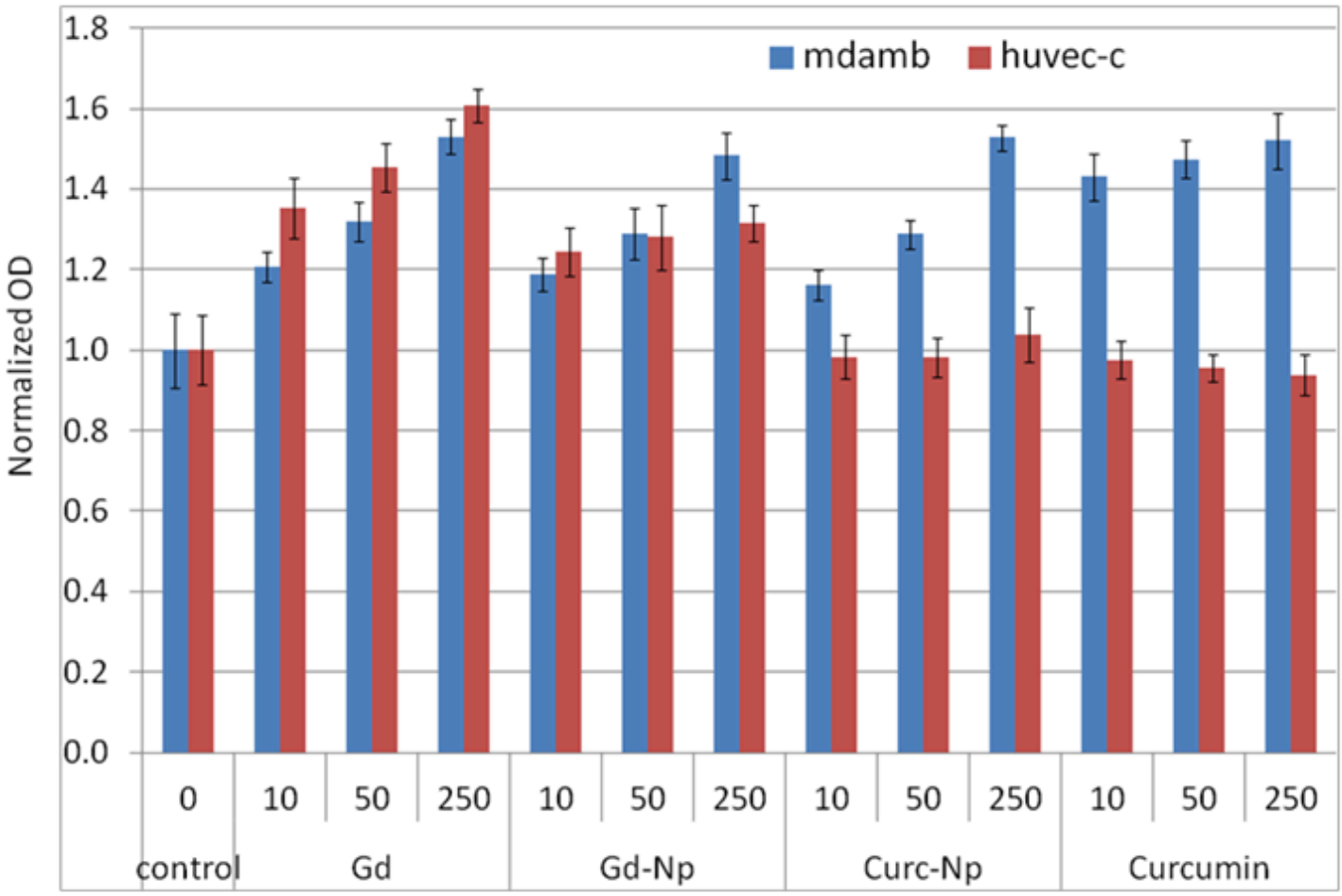



**Figure 7**

LDH assay

## Supplementary Files

This is a list of supplementary files associated with this preprint. Click to download.

- GraphicalAbstract.png